Research Article

Hydrodynamic simulation and experimental studies of an internally circulating bubbling fluidized bed with concentric cylinders

J.P. Simanjuntak[1,2], Z.A. Zainal[1,*], M.Z. Abdullah[1]
[1] School of Mechanical Engineering, Universiti Sains Malaysia, Engineering Campus, 14300 Nibong Tebal, Penang, Malaysia
[2] Mechanical Engineering Department, State University of Medan, Medan, 20221, North Sumatera, Indonesia

Received date: 21 February 2014, Accepted date: 9 May 2014

Academic Editor: Afşin Güngör

*Corresponding author. Tel.: +60 4 5937788; Fax: +60 4 5941025
E-mail address: mezainal@usm.my (Z.A. Zainal)

Abstract

This paper presents hydrodynamic simulation and experimental studies of gas–solid flow in an internally circulating bubbling fluidized bed (ICBFB) using concentric cylinders. An Eulerian–Eulerian Model (EEM) incorporating the kinetic theory of granular flow (KTGF) was applied in order to simulate the gas–solid flow behavior. The gas and solid dynamic was simulated using a computational fluid dynamics (CFD) software package, Fluent 6.3. Three–dimensional (3D) geometry was used to represent the key parts of a pilot scale of this reactor. Simulations were conducted to investigate the effect of the changes of six operating parameters: the fluidization flow rate of the draft tube (Q_{dt}), the aeration flow rate of the annulus (Q_{an}), the initial bed static height (H_{bs}), the draft tube height (H_{dt}), the draft tube diameter (D_{dt}), and the orifice diameter (D_{or}) on the solid flow characteristics in terms of the solid circulation rate (G_s). The results were then validated with the experimental results. All the investigated operating parameters have strong effect on G_s.

Keywords: Concentric cylinders fluidized bed; Solid circulation rate; Finite volume approach; ANSYS/Fluent

1. Introduction

Dual fluidized bed (DFB) is a fluidized bed configuration that consists of commonly two parallel interconnected chambers separated by an internal wall with an opening at the base and a common freeboard at the top with difference air stream velocities [1]. This configuration maintains the internal circulation of the bed particles within the system during operation. This fluidized bed is employed to avoid direct contact between the gasification and combustion processes so that the gaseous products (producer and flue gases) remain separated [2]. Therefore the quality and calorific value of the producer gas can be improved.

Controlling the bed particle circulation between the two chambers is critical because it influences the gasification process [3]. The DFB configuration has been studied for internal circulating ability of the bed particle for gasification process [4–8]. The highly endothermic gasification process is gained from the heat from the combustor where the char is combusted to produce heat and transported by the circulating hot material as heat carrier between the two reactors [9].

Internally circulating bubbling fluidized bed (ICBFB) consists of two concentric cylinders of different diameters. The inner cylinder also called the draft tube operates as a bubbling fluidized bed combustor. Whilst between the inner and outer cylinder is the annulus zone that operates as aerated bed gasifier. The two regions are connected via orifices at the bottom. This configuration is compact and has relatively low heat loss from the reactor compared to the DFB since the draft tube is located inside the annulus.

A similar configuration has been studied where a tube is placed in an annulus to divide the fluidized bed into two regions. This configuration is called as recirculation fluidized bed (RCFB) or a spouted bed with a central draft tube [10, 11]. However there is a difference between ICBFB and RCFB where the former has orifices instead of opening at the base. This will reduce gas bypass from the annulus to the draft tube or vice versa [12]. In addition to the heat transfer from the draft tube to the annulus zone via the bed material, the heat could also be transferred through the wall of the draft tube to the annulus zone.

Since the hydrodynamic state of the fluidized bed is influenced strongly by its configuration, several studies have used computational fluid dynamics (CFD) to determine the hydrodynamic characteristics in DFB [7, 8], but models for ICBFB in concentric cylinders are quite scarce. CFD modeling can aid and clarify any constraint on the real process with actual fluid properties in the fluidized bed. Thus a wide range of variations in the operational parameters can be tested and refined until a design that offers optimum performance is identified.

This paper presents the development of a cold–flow hydrodynamic study of an ICBFB with concentric cylinders using the CFD modeling of gas–solid flow and validated with experimental results. The contribution of the present study is that the Eulerian–Eulerian Model (EEM) is presented for a gas–solid two phase flow system.

This model has been used to carry out parametric investigation in CFB and DFB using CFD package ANSYS/Fluent [13, 14]. In this work, the EEM model was used to simulate the gas–solid flow in a pilot scale cold model ICBFB. With the aid of this model, the profiles of the bed pressure near the orifices and the solid velocity through the orifices were simulated and visualized. The effect of the various operating parameters on the hydrodynamic flow were assessed to improve the reactor design and to optimize the operating condition of this reactor. The main goal of this study is to explore the likely effect of different operating parameters on the bed behavior and the solid circulation rate.

2. Model description

2.1. Simulation model description

EEM allows for the modeling of gas–solid flow which treats both solid and gas phases as interpenetrating continua where the motion of each phase is solved using a suitable closure terms. A set of momentum and continuity equations along with its closure is solved using the finite volume approach, Fluent 6.3. The EEM takes relatively less computational time compare to discrete element method (DEM), but the accuracy depends on the closure equations (sub–models) and additional equation used. In this work, these sub–models are based on the kinetic theory of granular flow (KTGF) and used to enable calculation of solid phase pressure. The sub–models used in the present study is shown in Table 1 and similar to the work by Feng et al. [14].

Table 1. Sub–models used in this study.

Specific models	**Present study**	**Feng et al [14]**
Granular viscosity	Syamlal O'Brien	-
Granular bulk viscosity	Lun et al.	Lun et al.
Frictional viscosity	Schaefer	Schaefer
Frictional Pressure	Syamlal et al.	Lun et al.
Solid Pressure	Syamlal et al.	Syamlal et al.
Radial Distribution	Lun et al.	Lun et al.
Drag Model	Syamlal O'Brien	Gidaspow

2.2. Boundary condition and simulation parameters

At the gas inlet, the flow rates of the fluidizing and aerating gases were specified whilst the flow rate of the solid was set to zero. At the outlet, the pressure of both the gas and the particles were at an ambient condition. On the walls, no–slip wall conditions were assumed for both the gas and solid materials. This study was based on the available model implemented in Fluent 6.3 and values used for the parameters in the model are given in Table 2. Phase Couple Simple was used to control the solutions. First order upwind discretization scheme was used for the convection terms in the momentum equations, while the quadratic upwind interpolation (QUICK) scheme was used for the volume fraction equations. Syamlal O'Brien

model was used for the drag coefficient for solid phase. An iteration was taken for each time step to reduce the time during simulation.

Table 2. Simulation parameters.

Parameters	Value	Remarks
Particle density (ρ_p)	1520 kg/m^3	Quartz sand
Gas density (ρ_g)	1.2 kg/m^3	Air at ambient condition
Gas viscosity (μ)	1.79 x 10^{-5} Pa s	Air at ambient condition
Pressure (P)	101325 Pa	Atmospheric pressure
Restitution coefficient (e)	0.9	[15]
Internal friction angle (φ)	30^o	[14]
Solid volume fraction (α_s)	0.589	Set value
Time step (ΔT)	0.001 s	[14]

2.3. Simulation conditions

Fig. 1 shows the specific geometry of the concentric cylinders used in this work. The reactor has two inter–connected fluidized bed zones. The draft tube representing the combustion chamber has a diameter of 0.1 m and of 0.32 m height from the base. The annulus zone representing the gasification chamber has a diameter of 0.3 m. A dipleg with of 0.18 m diameter was placed 0.28 m from the base to avoid the gases from the two zones from mixing. The two zones were connected via orifices in the lower section of the draft tube to enable the solids to move from the annulus zone to the draft tube. The orifice diameters were 20 mm and located 80 mm above the air distributor plate which was used for uniform air supply to the draft tube. A conical plate with an inclination of 60^o relative to the horizontal plane was used for air supply to the annulus zone. This type of air distributor reduces stagnant region at the bottom of the bed. Tet/Hybrid elements were used to generate meshing to the geometry of the reactor with a 15 spacing interval size. There were a total of 447160 elements with a skewness value between 0.2 and 0.3.

The base geometry with total height 0.90 m as shown in Fig. 1 was used to investigate the effect of six operating parameters: the fluidization flow rate of the draft tube (Q_{dt}), the aeration flow rate of the annulus (Q_{an}), the initial bed static height (H_{bs}), the draft tube height (H_{dt}), the draft tube diameter (D_{dt}), and the orifice diameter (D_{or}) on the particle flow characteristics in terms of the solid circulation rate (G_s). Table 3 list the specific simulation cases of the 3D ICBFB used in this work. An iteration was taken for each time step and although desirable, grid independence study was not done to reduce the computational time during simulation.

Table 3. Simulation cases.

	Q_{dt} (lpm)	Q_{an} (lpm)	H_{bs} (mm)	D_{dt} (mm)	D_{or} (mm)	H_{dt} (mm)
Effect of Q_{dt} (Case-1)	300, 350, 400, 450	150	280	100	20	320
Effect of Q_{an}	350	50, 100, 150,	280	100	20	320

(Case-2)		200, 250				
Effect of H_{bs} (Case-3)	350	150	260, 300, 320	100	20	320
Effect of D_{dt} (Case-4)	350	150	280	75, 100, 125, 150	20	320
Effect of D_{or} (Case-5)	350	150	280	100	10, 15, 20, 25	320
Effect of H_{dt} (Case-6)	350	150	280	100	20	260, 280, 350, 370

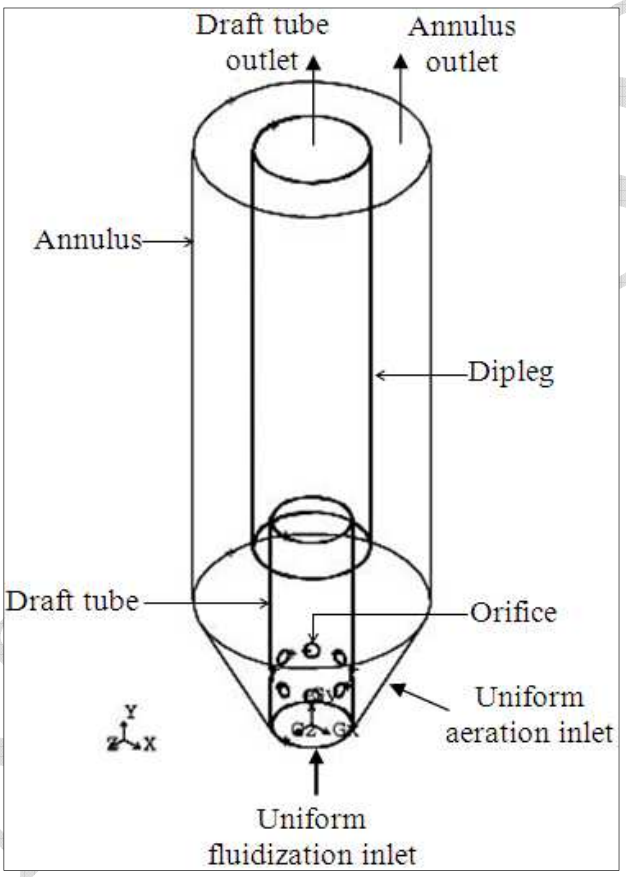

Fig. 1. Schematic drawing of the 3D ICBFB base case geometry

3. Experimental study

3.1. Apparatus set up

A pilot scale ICBFB with concentric cylinders was developed to validate the CFD model. A schematic diagram of the experimental set up is illustrated in Fig. 2. The main body of the ICBFB unit was made of plexiglas and consisted of two concentric cylinders, outer cylinder (1), inner cylinder (2). A dipleg (3) was installed between the inner and outer cylinders to prevent mixture of the gas streams from the two

chambers. The annulus has a 0.30 m I.D. and 0.70 m height with a centrally located draft tube (0.1 m I.D. and 0.32 m height) with eight orifices (4) of 0.02 m I.D drilled on the draft tube wall located 0.08 m above the distributor plate. Bubble caps with orifice (0.0025 m–I.D) were used as gas distributor mounted on an inclined plate in the annulus zone (5) and on a flat plate in the draft tube (6). There were two air plenums to supply gas into the draft tube (7) and the annulus (8) regions separately. The annulus zone and draft tube were filled with silica sand, Geldart group B particles with a mean diameter of 450 μm and a density of 1520 kg/m^3 (9) and fluidized by using an air blower (10), controlled by valves (11, 12) through air rotameters (14, 15). A metal screen (16) was used to collect the bed particle that overflows from the draft tube.

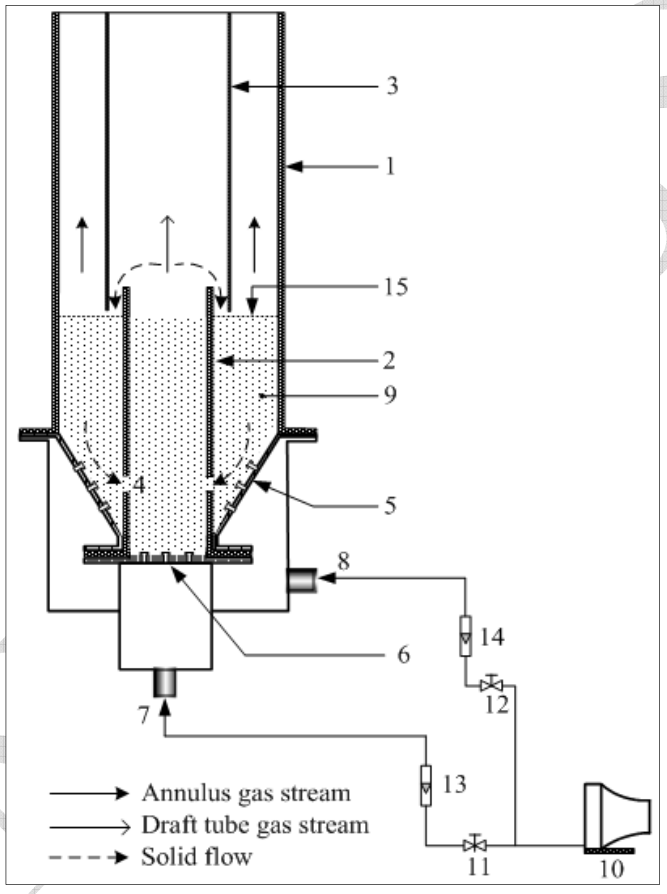

Fig. 2. Schematic diagram of the experimental set up.

Validation was conducted for case–1. Solid circulation rates were measured as a function of fluidization rate into the draft tube at constant aeration rate in the annulus as shown in Table 4. Maximum inventory of the bed particles was such that the annulus bed level never rose above the draft tube.

Table 4. Ranges of operating parameter used in the experimental.

Static bed height, H_{sb} (mm)	Fluidization rate, Q_{dt} (lpm)	Aeration rate, Q_{an} (lpm)
280	300–450	150

3.2. Measurement of solid circulation rate

Solid circulation rate is an important parameter and it affects the process in the ICBFB gasifier. Several researchers have measured the circulation rate of solid particles in RCFB using different methods. They measured the solid circulation rate through the particle downward velocity in the annulus. Most of the methods reported were either costly, involving high expertise and sophisticated equipment or time consuming. Particle downward velocity close to the wall were moving at velocities 20 to 80% lower than the particles farther away from the wall due to the wall effect [16]. Measurement of velocity on the wall was not done, but the effect is expected based on Rovero et al. [16]. A novel technique for direct measurement of solid circulation rate in a spouted bed has been implemented. It was done by collecting solids emerging from the top of the draft tube onto a screen over a period of time and weighed to obtain the circulation rate. The advantages of this method are direct measurement of the circulation rate, does not require sophisticated equipment and easy to perform the measurement. In this experimental study, the draft tube sizes (diameter and height) and angle of the inclined air distributor were fixed and were not easily changeable.

4. Results and discussion

4.1. Gas and solid flow hydrodynamic

Fig. 3 shows the instantaneous spatial distributions of the solid hold–up (solid volume fraction) in the Z–sliced planes in the ICBFB. A time–averaged value of 30 second simulation time was used to quantify the effect of those parameters on the solid flow dynamic of the system. The solid filled both the annulus and the draft tube at the same initial level at 280 mm from the air plate distributor. Q_{an} was held constant at 150 lpm, whereas Q_{dt} was varied from 300 lpm to 450 lpm.

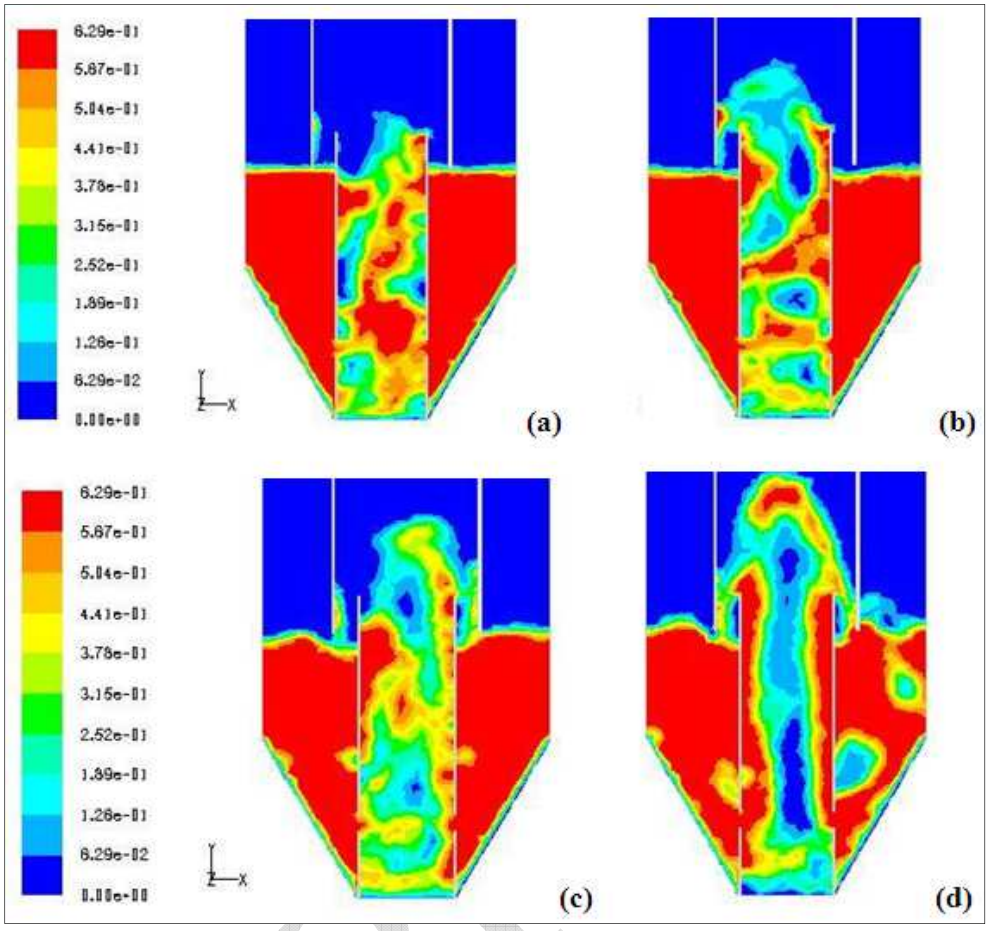

Fig. 3. Instantaneous snapshot of solid volume fraction distribution for the case–1: (a) Q_{dt} = 300 lpm; (b) Q_{dt} = 350 lpm; (c) Q_{dt} = 400 lpm; (d) Q_{dt} = 450 lpm.

As shown in Fig. 3, fluidization is more vigorous in the draft tube than in the annulus zone in all cases as demonstrated by the solid volume fraction distribution. For an ICBFB with two interconnected fluidized bed zones, the bed pressure is closely related to the solid hold–up between the two zones. The ΔP between the two zones provides a driving force for the solid and gas flow from the annulus zone to the draft tube through the orifices. The bed pressure distribution in both the annulus zone and the draft tube of Fig. 3(b) is shown in Fig. 4.

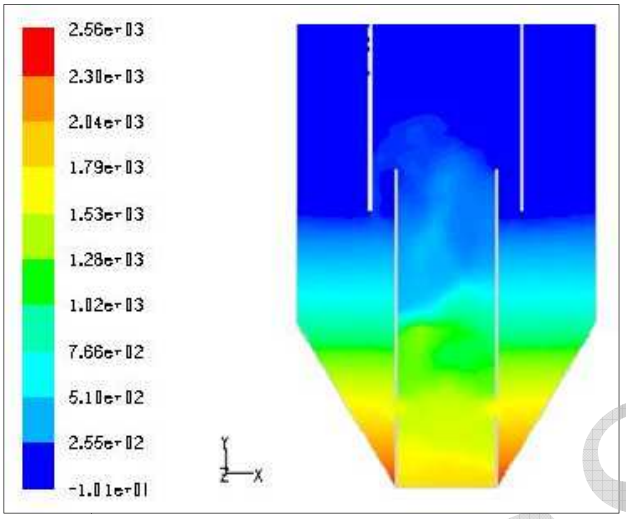

Fig. 4. Spatial distribution of the bed pressure for the base case–1 of Fig. 3(b).

Fig. 5 plots the average value of the bed pressure in the annulus zone and the draft tube along the orifice. The periodic vigorous bubbling of the bed materials inside the draft tube leads to fluctuations in the bed pressure.

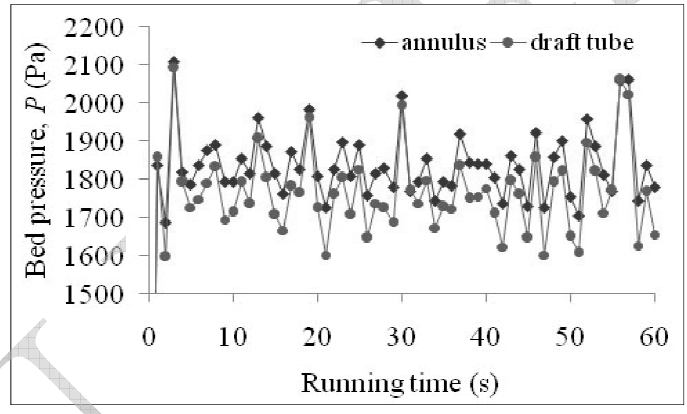

Fig. 5. Variations of the bed pressure with time in the draft tube and the annulus around the orifice for the base case-1 of Fig. 3(b).

Profile of bed pressure in the annulus zone and the draft tube on the Y–axis and across the orifice on radial–axis are plotted in Figs. 6a and 6b respectively. As can be seen, the annulus zone has a higher pressure than in the draft tube around the orifices, which causes the solid to move from the annulus zone to the draft tube. At the top of the draft tube the pressure is higher than in the annulus zone, and this causes the solid to overflow into the annulus zone, as illustrated in Fig. 6a.

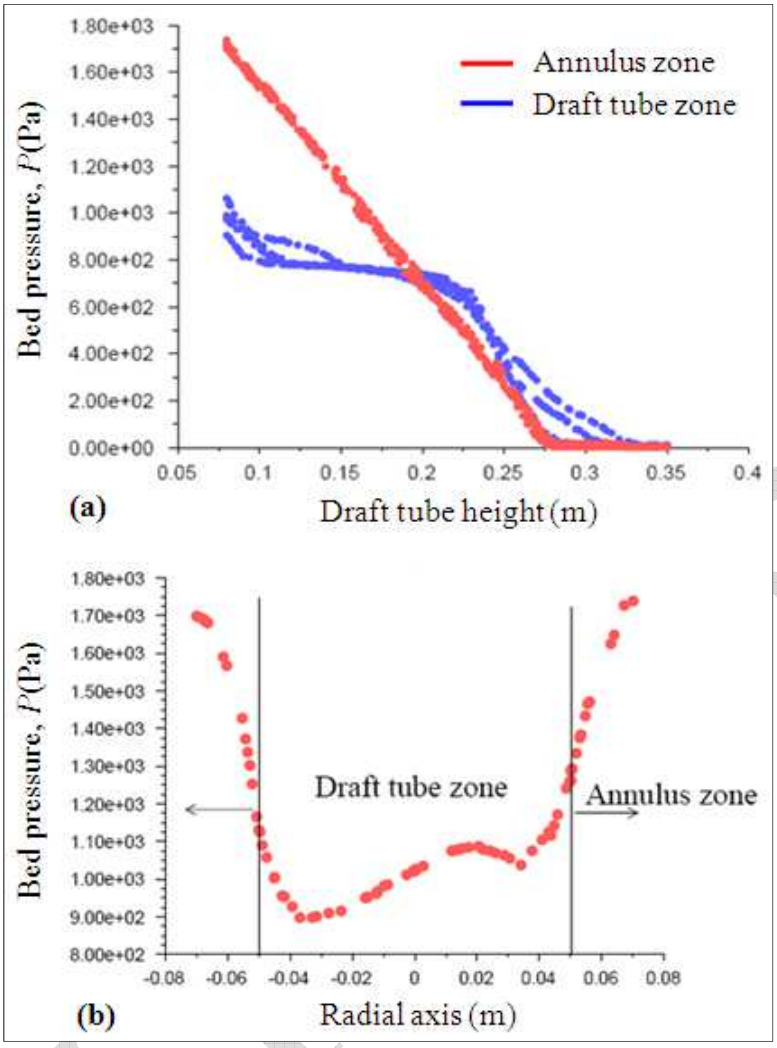

Fig. 6. Bed pressure profile for the base case-1 of Fig. 3(b): (a) Along the draft tube height; (b) Along radial axis near the orifice.

4.2. Solid circulation rate (G_s)

The mechanism governing of the solid circulation in the ICBFB is explained based on the gas and solid dynamics obtained from the simulations. The effect of six operating parameters: Q_{dt}, Q_{an}, H_{bs}, H_{dt}, D_{dt}, and D_{or} on G_s were analyzed within the system. G_s was computed by the following equation: $G_s = (1-\varepsilon_f)\,\rho_s\,U_{s,av}\,A_o$, where ε_f, $U_{s,av}$, ρ_s and A_o are the voidage, average solid velocity magnitude through the orifices, solid density, and orifice area respectively. The voidage ε_f is equal to ε_{mf} based on the assumption that when the fluidized material flows through the orifice between the high flow rate zone and the low flow rate zone, the cross flow rate of the fluidizing medium is very small and can therefore be neglected. $U_{s,av}$ is determined from the solid average velocity magnitude through the orifices as shown in Fig. 7.

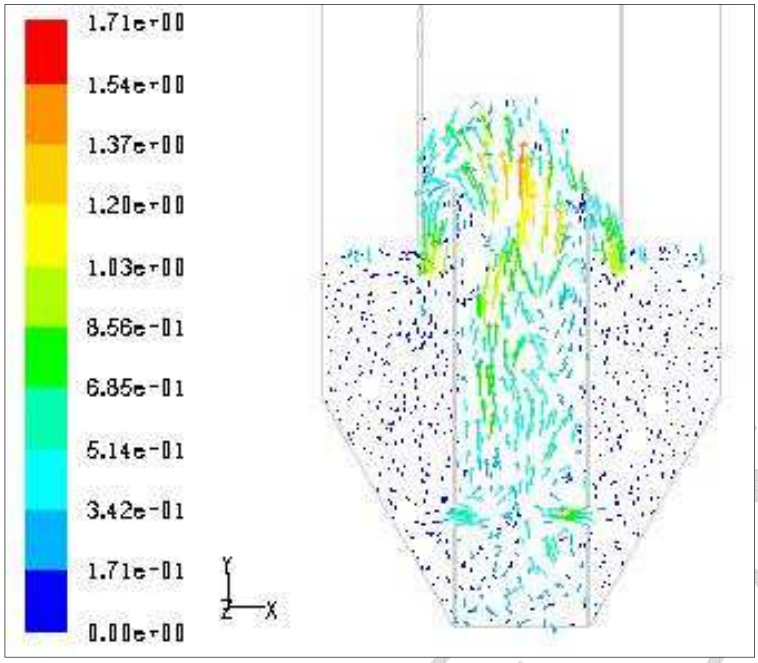

Fig. 7. Solid velocity vector for the base case-1 of Fig. 3(b).

4.3. Effect of Q_{dt} on ΔP

Fig. 8 shows the average value of ΔP between the annulus zone and the draft tube near the orifices at H_{bs} = 280 mm. ΔP increased when Q_{dt} was increased from 300 lpm to 450 lpm whilst maintaining Q_{an} 150 lpm. This is due to the flow regime in the draft tube that changed from bubbling regime to vigorous bubbling flow regime, which reduces the solid hold–up and resulted in a distinct pressure reduction in the draft tube zone. The annulus zone lies in the moving bed state with a high solid hold–up, which results in the relative constant pressure.

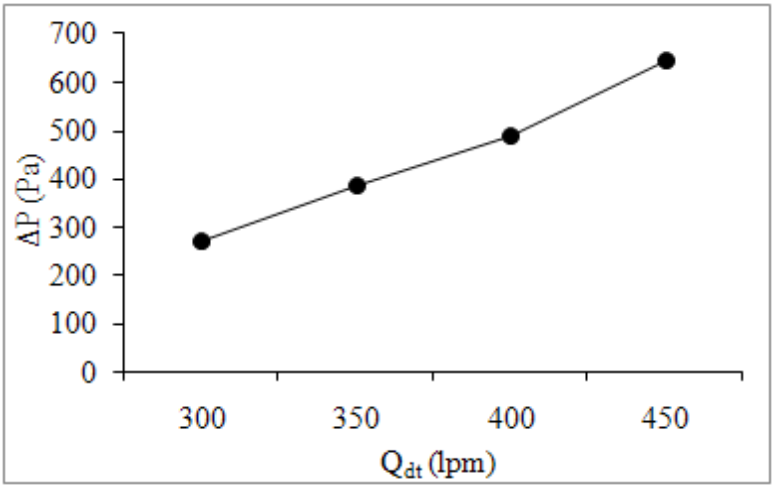

Fig. 8. Effect of Q_{dt} on ΔP for the base case–1.

4.4. *Effect of Q_{an} and Q_{dt} on G_s*

The effects of Q_{an} and Q_{dt} on G_s in the simulation study are shown in Fig. 9. Initially G_s increased as Q_{an} was increased, however G_s decreased when Q_{an} was further increased to 200 lpm and 250 lpm respectively. The trend is consistent with previous experimental findings [4, 14]. A detailed quantitative comparison cannot be made because the geometrical for the cases are different.

In Fig. 9 G_s increased when Q_{an} was increased from 50 lpm to 150 lpm as a result of the increase in ΔP across the orifices as shown in Fig. 8. At 50 lpm Q_{an}, the solid circulation was low because Q_{an} is much smaller than the minimum fluidization flow rate (Q_{mf} = 150 lpm). Consequently the bed materials in the annulus zone were packed more densely and entered the draft tube slowly.

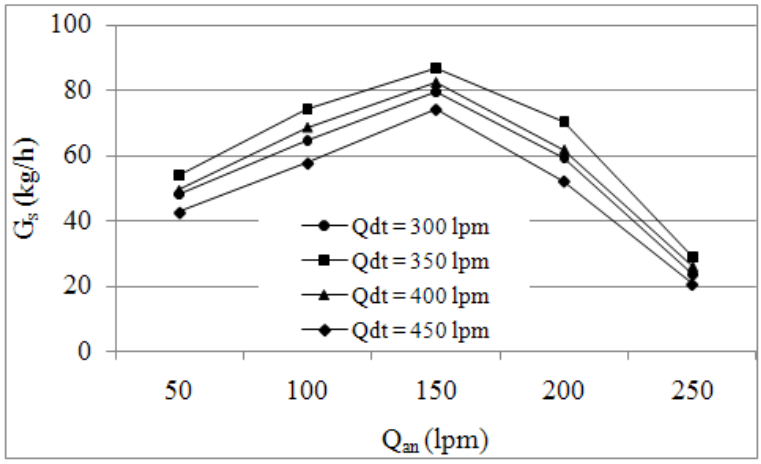

Fig. 9. Effect of Q_{an} and Q_{dt} (cases-1 and 2) on G_s in the simulation

However, G_s increased when Q_{an} was increased up to the Q_{mf} due to the active movement of solid particles with increasing ΔP. This finding is similar to previous work [12, 14]. With increasing Q_{an}, the solid particles in the annulus section are close to the minimum fluidizing state. Therefore the diluted density of the annulus bed decreased as ΔP near the orifice was increased, which led to easier solid movement into the draft tube and consequently increases G_s. G_s then decreases when Q_{an} is greater than 150 lpm, because at this condition bubbles start to form which leads to a decrease in the bed density in the annulus zone. A higher rate of aeration in the annulus causes a reduction in the bed density and ΔP between the annulus zone near the orifice, which results in a lower G_s.

Fig. 9 also describes the effect of Q_{dt} on G_s where G_s increased slightly when Q_{dt} was increased from 300 lpm to 350 lpm due to the increase in the driving force between the two beds. Increasing Q_{dt} increases the bed voidage in the draft tube. The low bulk density of the draft tube and a higher ΔP across the orifices led to a higher G_s. However, a higher Q_{dt} (above 350 lpm) did not improve G_s although ΔP was higher as illustrated in Fig. 8. This was due to two opposite influences on G_s by Q_{dt}. In one aspect, with the increase in Q_{dt}, the diluted density of the draft tube decreased and

ΔP at the orifice increased and led to a higher G_s. In another aspect, a Q_{dt} which is too high enhanced bubbling near the orifice and hindered solid flow into the draft tube. Increasing Q_{dt} caused a larger fraction of the bubbles in the void fraction near the orifice and hindered the solid flow into the draft tube leading to a reduction in G_s. However, solid circulation did not occur until the gas flow rate in the draft tube reached $2Q_{mf}$, even if the gas velocity to the annulus section was sufficiently high.

4.5. Effect of sizes geometry on solid circulation

4.5.1. Effect of static bed height (H_{bs})

H_{bs} had strong effect on G_s. Fig. 10a shows that G_s increased with H_{bs}. When H_{bs} was low, fluidization in the draft tube was below H_{dt}, thus there was no bed particle overflow from the draft tube to the annulus zone. This led to low solid circulation between the two zones. It is of interest to determine how G_s is affected by H_{bs}. There is a minimum H_{bs} related to H_{dt} to initiate solid circulation in the system. It is expected that the effect of H_{bs} varies for the constant ratios of Q_{dt} to Q_{an}. In this study, Q_{an} and Q_{dt} were set at 150 lpm and 350 lpm respectively. Four H_{bs} were selected for comparison, which were 81.25%, 87.5%, 93.75% and 100% H_{dt}. A maximum value occurred when H_{bs} was at 280 mm which was the same as the height of the dipleg bottom. After that G_s reduced with H_{bs}.

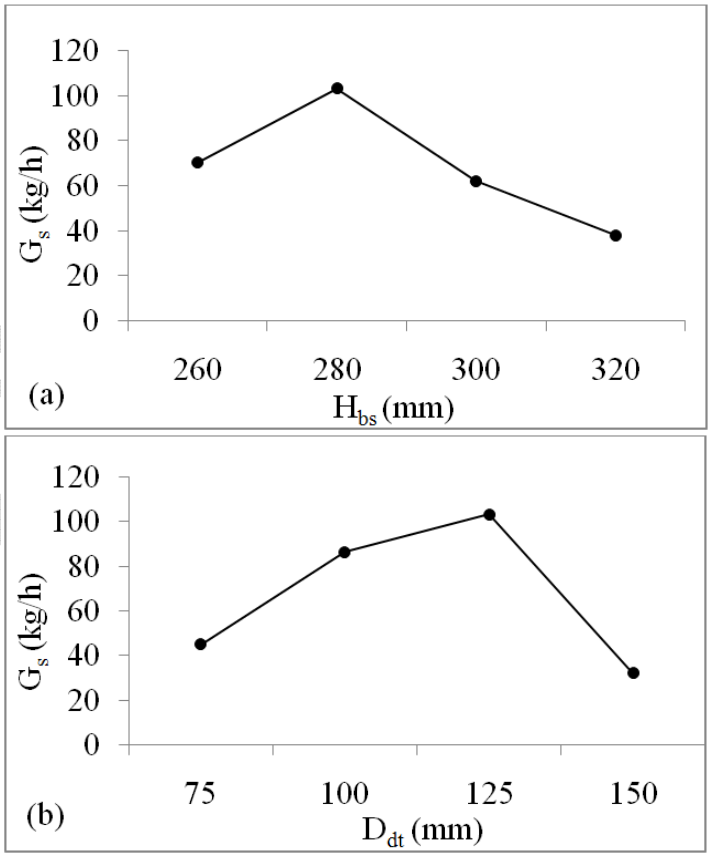

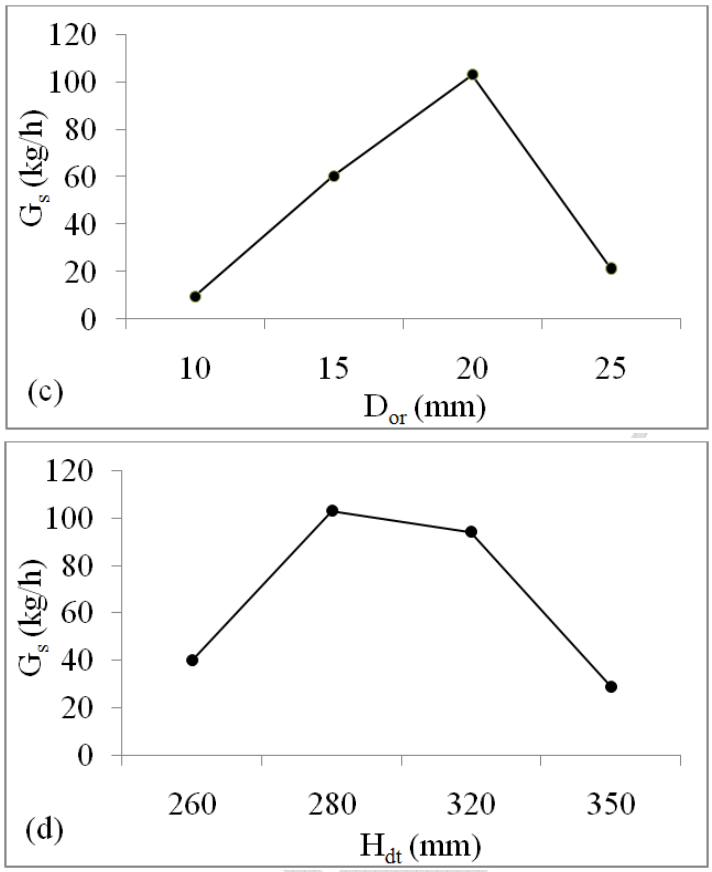

Fig. 10. Effect of sizes geometry on G_s: (a) Effect of H_{bs} (case–3); (b) Effect of D_{dt} (case–4); (c) Effect of D_{or} (case–5); (d) Effect of H_{dt} (case–6).

4.5.2. Effect of draft tube diameter (D_{dt})

The effect of D_{dt} on G_s is shown in Fig. 10b. The highest G_s occurred at D_{dt} = 125 mm when D_{dt} increased from 75 mm to 150 mm. This is due to the resistance to the solids between the annulus zone and the draft tube. By increasing or decreasing D_{dt}, the cross–sectional area of both the annulus and the draft tube also increases or decreases respectively. A larger D_{dt} resulted in a larger amount of solids into the draft tube, which requires a much higher gas flow rate and increases the bed density in the annulus. Consequently, a more vigorous collision occurs among the particles in the draft tube, and as a result the gas flow to the annulus decreases, while the gas flow to the draft tube increases.

4.5.3. Effect of orifice diameter (D_{or})

The type of connecting holes between the two zones in an ICBFB is very important for solid circulation. Since the pressure at the bottom of the draft tube was lower than that at the bottom of the annulus, some of the inlet gas to the annulus tends to bypass to the draft tube side. However, reverse gas bypassing from the draft tube to annulus is also possible.

Fig. 10c shows the effect of D_{or} on G_s. D_{or} which clearly shows a strong influence on G_s by increasing the orifice size. The area for solid particle passage also increases, and this decreases the solid flow resistance. Therefore G_s increases with increasing D_{or} due to a reduction in the solid flow resistance. These results are similar to those of previous reports [14]. When D_{or} is small (10 mm in this study), the solids form a cluster in the annulus zone near at the orifices and resists the gas flow from the draft tube into the annulus zone with a slow movement of the solids through the orifices. By further increasing D_{or} (15 mm), the phenomenon of the solid cluster at the annulus zone near the orifices became less severe. As a result, gas bypass from the draft tube into the annulus zone increased and the solid resistance significantly decreased. However, the velocity of the particles passing through the orifices decreased by increasing D_{or} from 20 mm to 25 mm. Due to the high inlet flow rate into the draft tube, the solid cluster phenomenon near the orifices vanished. Hence gas bypass into the annulus zone increased sharply and restrained the solid flow into the draft tube. As a result, G_s decreased significantly.

4.5.4. Effect of draft tube height (H_{dt})

The effect of varying H_{dt} on G_s was studied and is shown in Fig. 10d. H_{bs} was kept constant at 280 mm from the plate distributor and was always below the top of the draft tube for all draft tube heights. The minimum bed level (inventory of the solid) that can initiate solid circulation in the system was different for different H_{dt} when the other parameters were kept constant. As H_{dt} increased, the minimum H_{bs} required to cause solid circulation also increased considerably. Due to this reason it was only possible in a few cases to compare the G_s for the same H_{bs} for different values of H_{dt} while keeping the other parameters constant.

In this study, the shortest H_{dt} tested was 280 mm, which was the same as H_{bs}. Fig. 10d shows that G_s decreased with H_{dt} due to the friction between the particles and the wall of the draft tube. A higher H_{dt} causes higher friction. A higher H_{dt} requires much more energy to fluidize the solid from the draft tube into the freeboard, thus G_s decreased significantly. For the same H_{dt} in the annulus above the distributor plate, G_s was lower for longer draft tubes.

For the highest draft tube (H_{dt} = 370 mm) a reversal solid circulation from the draft tube to the annulus zone via the orifice was observed. Again, this is due to the solid resistance between the annulus and the draft tube. The higher the draft tube, the larger the resistance. Thus not much solid can reach the top of the draft tube and part of it sinks and flows back into the draft tube due to gravity. The bed pressure in the draft tube becomes higher than in the annulus as illustrated in Fig. 11. Therefore solid flows from the draft tube into the annulus zone through the orifices.

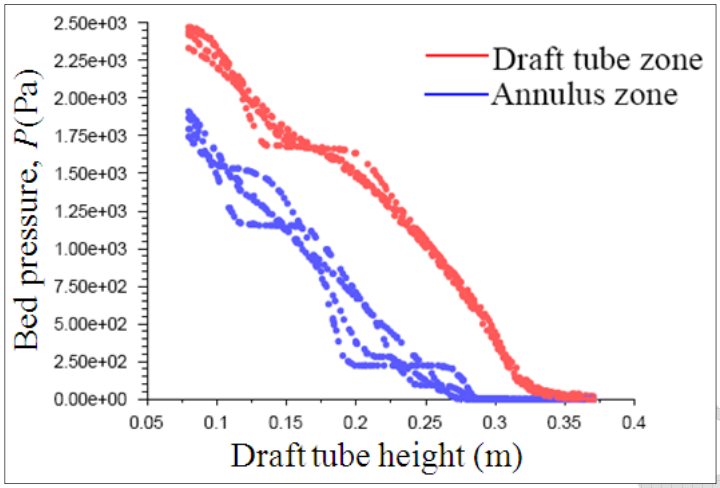

Fig. 11. Bed pressure profile on case–6 at 370 mm H_{dt}.

5. Experimental validation

Results show that solids in the annulus section were in the fixed bed state and did not circulate at Q_{an}<50 lpm. Solid circulation rate reached a maximum value at Q_{an} = Q_{mf}. Fig. 12 shows the solid circulation rate from the CFD modeling and experimental work for case-1 at 150 lpm Q_{an}. Maximum circulation rate predicted by the simulation was within 5% of the experimental results. However solid circulation rate from experiments were always lower than predicted by the model. In the experiment, wall effect tends to reduce the particle downward velocity in the annulus zone [16, 17] or even became stagnant. In addition, resistance to the solid flow through the orifices resulted in decrease of the solid velocity thus reducing the solid circulation [18].

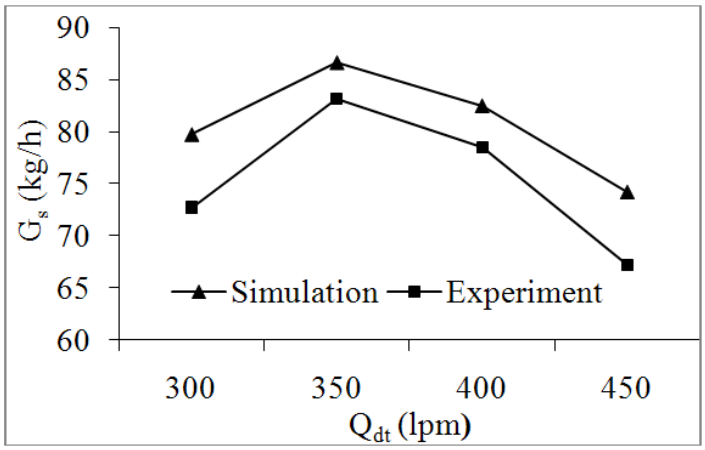

Fig. 12. Solid circulation comparison of simulation and experiment (case–1).

6. Conclusions

The solid flow dynamic in the ICBFB with concentric cylinders was investigated using the EEM incorporating the KTGF. Commercial CFD software, Fluent 6.3 was

used as the numerical iterative method for the simulation. Effects of six operating parameters on the solid–gas hydrodynamic were investigated. The simulation results demonstrate that the CFD model can predict well the solid–gas hydrodynamic in the ICBFB system for all six parameter runs. Results show that the solid flow from the annulus to the draft tube through orifices was caused by the ΔP between them as the driving force. Amongst the parameters investigated, Q_{dt}, and Q_{an} had the most significant effect on G_s.

Acknowledgments

The financial support provided by PRGS, Universiti Sains Malaysia as a research grant (No. 1001/PMEKANIK/8042040) is gratefully acknowledged. One of the authors (J.P. Simanjuntak) would also like to thank the Directorate General of Higher Education (DGHE), Ministry of Education and Culture (MOEC) Republic of Indonesia, under second batch of the Overseas Postgraduate Scholarship Program.

References

1. Kuramoto, M., D. Kunii, and T. Furusawa, *Flow of dense fluidized particles through an opening in a circulation system.* Powder Technology, 1986. 47(2): p. 141-149.
2. Loffler, G., et al., *Hydrodynamics of a dual fluidized-bed gasifier Part I: simulation of a riser with gas injection and diffuser.* Chemical Engineering Science, 2003. 58(18): p. 4197-4213.
3. Murakami, T., et al., *Some process fundamentals of biomass gasification in dual fluidized bed.* Fuel, 2007. 86(1-2): p. 244-255.
4. Fang, M., et al., *Experimental research on solid circulation in a twin fluidized bed system.* Chemical Engineering Journal, 2003. 94(3): p. 171-178.
5. Foscolo, P., et al., *Design and cold model testing of a biomass gasifier consisting of two interconnected fluidized beds.* Powder Technology, 2007. 173(3): p. 179-188.
6. Zhou, Z.-q., et al., *Study on biomass circulation and gasification performance in a clapboard-type internal circulating fluidized bed gasifier.* Biotechnology Advances, 2009. 27(5): p. 612-615.
7. Luo, K., et al., *LES–DEM investigation of an internally circulating fluidized bed: Effects of gas and solid properties.* Chemical Engineering Journal, 2013. 228(0): p. 583-595.
8. Xiao, X., et al., *Multi-stage biomass gasification in Internally Circulating Fluidized-bed Gasifier (ICFG): Test operation of animal-waste-derived biomass and parametric investigation at low temperature.* Fuel Processing Technology, 2010. 91(8): p. 895-902.
9. Corella, J., J. Toledo, and G. Molina, *Biomass gasification with pure steam in fluidised bed: 12 variables that affect the effectiveness of the biomass gasifier.* International Journal of Oil, Gas and Coal Technology, 2008. 1(1): p. 194-207.

10. Berruti, F., J. Muir, and L. Behie, *Solids circulation in a spout-fluid bed with draft tube.* The Canadian Journal of Chemical Engineering, 1988. 66(6): p. 919-923.
11. Song, B., Y. Kim, and S. Kim, *Circulation of solids and gas bypassing in an internally circulating fluidized bed with a draft tube.* Chemical Engineering Journal, 1997. 68(2-3): p. 115-122.
12. Zhang, H., et al., *Hydrodynamics of a novel biomass autothermal fast pyrolysis reactor: Solid circulation rate and gas bypassing.* Chemical Engineering Journal, 2012. 181–182(0): p. 685-693.
13. Mathiensen, V., Solberg, T., Hjertager, B.H. *An experimental and computational study of multiphase flow behavior in a circulating fluidized bed*. International Journal of Multiphase Flow, 2000. 26: p. 387-419.
14. Feng, Y., et al., *CFD modeling of gas-solid flow in an internally circulating fluidized bed.* Powder Technology, 2012. 219: p. 78-85.
15. Ding, J. and D. Gidaspow, *A bubbling fluidization model using kinetic theory of granular flow.* AIChE Journal, 1990. 36(4): p. 523-538.
16. Rovero, G., N. Piccinini, and A. Lupo, *Particles Velocity in Full and Semicylindrical Sprouted Bed.* Vitesses des particulales dans les list a jet tri-dimensionels et semi cylindriques, 1985. 21(124): p. 43-49.
17. Yang, W. and D. Keairns. *Recirculating fluidized bed reactor data utilizing a two-dimensional cold model*. in *AIChE Symp. Ser*. 1974.
18. Tallon, S. and C. Davies, *Discharge of a fluidised bed of particles through an orifice.* Powder Technology, 2005. 160(1): p. 45-53.